$\mathcal{O}(N \log N)$ scaling method to evaluate the ion–electron potential of crystalline solids

Xuecheng Shao,[a] Wenhui Mi,[a] Qiang Xu, Yanchao Wang,[b] and Yanming Ma[c]
State Key Laboratory of Superhard Materials, Jilin University, Changchun 130012, People's Republic of China

(Received 12 June 2016; accepted 25 October 2016; published online 11 November 2016)

We propose a simple $\mathcal{O}(N \log N)$ scaling expression in reciprocal space for evaluating the ion–electron potential of crystalline solids. The expression replaces the long-range ion–electron potential with an equivalent localized charge distribution and corresponding boundary conditions on the unit cell. Given that no quadratic scaling structure factor is required—as used in traditional methods—the expression shows the inherent $\mathcal{O}(N \log N)$ behavior, and is well suited to simulating large-scale systems within orbital-free density functional theory. The scheme is implemented in the ATLAS software package and benchmarked by using a solid Mg body-centered cubic lattice containing tens of thousands of atoms in the unit cell. The test results show that the method can efficiently simulate large scale crystals with high computational accuracy. *Published by AIP Publishing.* [http://dx.doi.org/10.1063/1.4967319]

I. INTRODUCTION

Ab initio simulations of materials have become routine in the recent years, largely due to the success of density functional theory (DFT).[1,2] However, the conventional cubic-scaling Kohn-Sham DFT (KS-DFT) is limited to relatively small systems with unit cells of up to only thousands of atoms,[3] and is inappropriate for simulating many atomistic processes—for example, fracture or the dynamics of dislocation interactions—where realism is only achieved by considering millions of atoms. Such large-scale simulations are beyond KS-DFT, and require a linear scaling quantum mechanics method. The inherent quasi-linear scaling of orbital-free DFT (OF-DFT) makes it the most promising theory for large-scale simulations.[4,5] In general, all the interaction terms of OF-DFT have linear scaling except for the electrostatic interaction term for periodic systems.[6,7] The evaluation of the electrostatic potential therefore is the bottleneck in most OF-DFT programs.[6,7]

Generally, the electrostatic potential can be written as the sum of ion–ion, electron–electron, and ion–electron terms. In a periodic system, each of these terms diverges due to the long-range $1/r$ nature of the Coulomb interaction.[8–12] Divergences that are conditional convergences of extended lattice summations can be eliminated by formulating the summations in terms of neutral densities that are well localized in real/reciprocal space.[13]

The ion–ion term can be transformed to a standard Ewald summation[13] under periodic boundary conditions (PBCs), which scales as $\mathcal{O}(M^2)$, where M is the number of atoms in the system. Particularly, the particle mesh Ewald method[14,15] was proposed as $\mathcal{O}(M \log M)$ scaling for evaluation of the ion–ion term. The computational cost of this term is acceptable for OF-DFT calculations of large systems. The electron–electron term can be convoluted in reciprocal space with $\mathcal{O}(N \log N)$ scaling under PBCs, where N is the number of grid points in the system, making its computational cost also acceptable for large-scale simulations. However, the computational cost of the ion–electron potential term of crystalline solids scales as $\mathcal{O}(N \cdot M)$ in reciprocal space due to the requirement of calculation of the structure factor.[6,7,16] Given that the number of grid points generally scales linearly with the number of ions, the computational cost of the ion–electron term is effectively $\mathcal{O}(N \cdot M)$ scaling. Note that N is much larger than M, and the computation of structure factor is time-consuming. Therefore, the ion–electron term dominates the computational time in OF-DFT calculations for large systems.[6,7,16]

II. THEORY AND BACKGROUND

Two methods with much better scaling have been proposed to calculate the ion–electron potential in reciprocal and real space. In reciprocal-space representation, the cardinal B-spline approximation mathematical technique was employed to significantly reduce the computational cost of calculating the structure factor for large periodic systems.[16] The method exhibits linear scaling, and has been successfully applied to systems containing 1×10^6 atoms in the simulated cell.[16] In real space representation, a method has been proposed to replace the infinite sum of the long-range Coulomb potential by equivalent localized charge distributions and PBCs. Given the localized charge distributions and the boundary conditions, the summations of all the terms of the electrostatic potential can be evaluated by solving the corresponding Poisson equation.[12]

Note that the long-range Coulomb potential can be represented as localized "ion charge" and the corresponding boundary conditions in the real-space based method.[12] Based on this fact, we propose an alternative $\mathcal{O}(N \log N)$ scaling scheme to evaluate the ion–electron potential term of crystalline solids in reciprocal space. Our method can avoid calculation of the structure factor, and thus the method exhibits much better scaling. In the pseudopotential approximation, the total ion–electron potential V_{i-e} of a crystal can be expressed in real

[a]X. Shao and W. Mi contributed equally to this work.
[b]Electronic mail: wyc@calypso.cn
[c]Electronic mail: mym@calypso.cn

22 January 2024 16:56:14

space $V_{i-e}(\boldsymbol{r})$ or reciprocal space $V_{i-e}(\boldsymbol{G})$. Note that $V_{i-e}(\boldsymbol{r})$ can be simply evaluated by $V_{i-e}(\boldsymbol{G})$ with the fast Fourier transform (FFT), which is an $\mathcal{O}(N \log N)$ operation.[17] Therefore, we focus on the expression of ion–electron potential only in reciprocal space. For a given periodic system with n atomic species, the total ion–electron potential $V_{\text{i-e}}$ can be expressed in reciprocal space as[7,18]

$$V_{\text{i-e}}(\boldsymbol{G}) = \frac{1}{\Omega}\sum_{k=1}^{n} S^k(\boldsymbol{G}) V^k_{\text{loc}}(\boldsymbol{G}), \tag{1}$$

where Ω is the volume of the unit cell, V^k_{loc} is ionic pseudopotential, and the structure factor of the kth atomic species $S^k(\boldsymbol{G})$ is given as

$$S^k(\boldsymbol{G}) = \sum_{j=1}^{n^k} \exp(i\boldsymbol{G}\cdot\boldsymbol{r}_{k,j}), \tag{2}$$

where n^k and $\boldsymbol{r}_{k,j}$ are the number of atoms and the position of the jth atom of kth atomic species, respectively. The term G is determined by the primitive vectors of reciprocal space $\boldsymbol{b}_i$ (i.e., $\boldsymbol{G} = n_1\boldsymbol{b}_1 + n_2\boldsymbol{b}_2 + n_3\boldsymbol{b}_3$, where n_i are integers). The evaluation of the structure factor in this expression scales as $\mathcal{O}(N \cdot M)$.

The local ionic potential of the kth atomic species $V^k_{\text{loc}}(r)$ can be represented by the pseudo-charge density $\rho_k(r)$, which can be used to reproduce the equivalent long-range ionic potential. The pseudo-charge density, $\rho_k(r)$, is only localized within the cutoff radius, r^k_c. Fig. 1 shows a typical local ionic pseudopotential and the corresponding pseudo-charge density of Mg, in which the cutoff radius is 2.6 a.u. The spherical symmetry makes the pseudo-charge density

$$\rho_k(r) = \frac{1}{4\pi}\left(\frac{2}{r}\frac{\partial}{\partial r} + \frac{\partial^2}{\partial r^2}\right) V^k_{\text{loc}}(r). \tag{3}$$

Here the numerical representation of $V^k_{\text{loc}}(r)$ is on a log grid and the triple-order polynomial fitting scheme is employed to estimate the pseudo-charge density. Note that the $\rho_k(r = 0)$ has the same value as its adjacent point to make pseudo-charge distribution continuous and smooth at boundary(r = 0).

To eliminate the evaluation of the structure factor, the total ion–electron potential $V_{i-e}(\boldsymbol{G})$ can be obtained by the total ionic charge density, $\rho_I(\boldsymbol{r})$, and the corresponding PBCs. The total ionic charge density can be estimated by summation of all the pseudo-charge density in unit cell

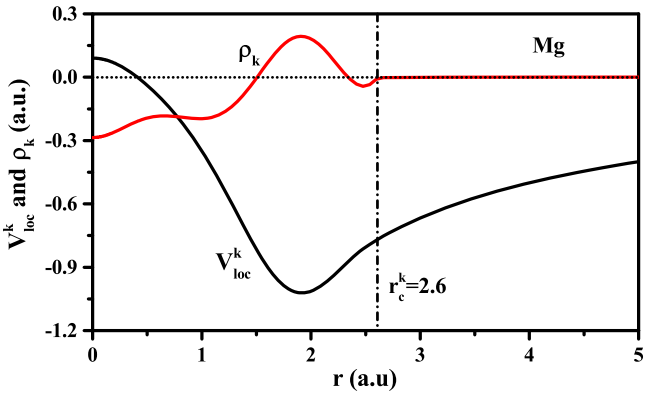

FIG. 1. Local pseudopotential and the corresponding pseudo-charge density.

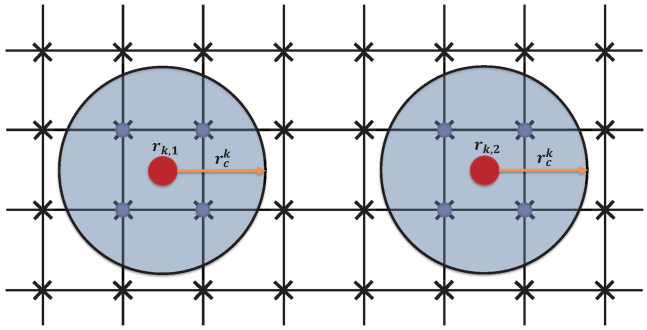

FIG. 2. The sketch of ionic charge distribution on grid points.

$$\rho_I(\boldsymbol{r}) = \sum_{k=1}^{n}\sum_{j=1}^{n^k} \rho_k(R_{k,j}). \tag{4}$$

Here, $R_{k,j} = |\boldsymbol{r} - \boldsymbol{r}_{k,j}|$. In principle, if $\rho_I(\boldsymbol{r})$ of each point is obtained by considering contributions of all atoms, the computational cost of $\rho_I(\boldsymbol{r})$ is $\mathcal{O}(N \cdot M)$ scaling. However, the pseudo-charge obtained from local pseudo-potential must be localized within the cutoff radius and no overlap for each atomic core (see Fig. 2), owning to the first-principle pseudopotentials should have strict Coulombic tail. Therefore, the $\rho_I(\boldsymbol{r})$ is determined by not more than one atom. Obviously, Eq. (4) is transformed to following equations:

$$\rho_I(\boldsymbol{r}) = \begin{cases} \rho_k(R_{k,j}) & (R_{k,j} \le r^k_c), \\ 0 & (R_{k,j} > r^k_c). \end{cases} \tag{5}$$

Thus, the expression for total ionic charge density $\rho_I(\boldsymbol{r})$ is linear scaling.

$\rho_I(\boldsymbol{r})$ can be used to evaluate the total ion–electron potential in real space $V_{i-e}(\boldsymbol{r})$ by solving a Poisson equation with the PBCs. However, the most convenient way to obtain the ion-electron potential in reciprocal-space is by

$$V_{i-e}(\boldsymbol{G}) = \begin{cases} \dfrac{4\pi\rho_I(\boldsymbol{G})}{|\boldsymbol{G}|^2} & (G \ne 0), \\ V_{i-e}(G) & (G = 0), \end{cases} \tag{6}$$

where $\rho_I(\boldsymbol{G})$ can be obtained by the FFT,

$$\rho_I(\boldsymbol{G}) = FFT(\rho_I(\boldsymbol{r})). \tag{7}$$

Just as in the conventional reciprocal method,[6,7,18] our method also shows the divergent problem for evaluating ion–electron energy for a charge-neutral periodic system. The problem can be neglected, because the singularity at $G = 0$ is canceled exactly by similar divergences in other electrostatic-interaction terms (the ion–ion and electron–electron interactions) in the reciprocal-space representation.[6,7,18] The same technique used in the conventional reciprocal method is employed in our scheme. Particularly, the $V_{i-e}(G = 0)$ term in Eq. (1) can be expressed in reciprocal space as

$$\begin{aligned} V_{i-e}(G = 0) &= \frac{1}{\Omega}\sum_{k=1}^{n} S^k(G = 0) V^k_{\text{loc}}(G = 0), \\ &= \frac{1}{\Omega}\sum_{k=1}^{n} n^k V^k_{\text{loc}}(G = 0), \end{aligned} \tag{8}$$

where n^k and $V^k_{\text{loc}}(G = 0)$ are the number of atoms and the local ionic potential of the kth atomic species, respectively.

22 January 2024 16:56:14

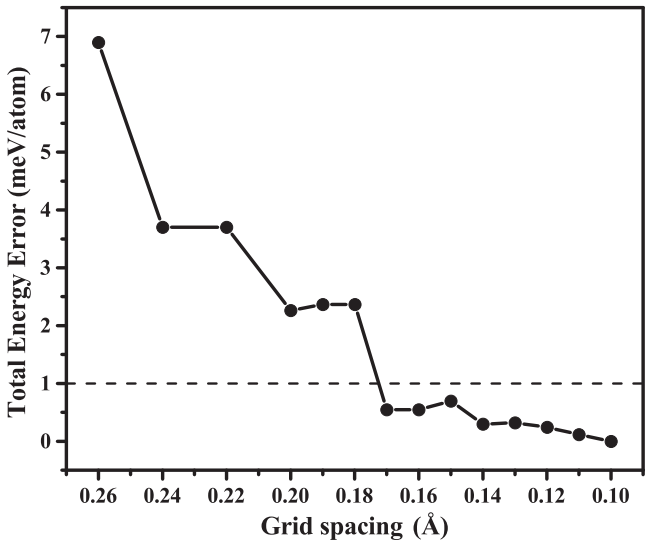

FIG. 3. Convergence of the total energy of bulk bcc Mg (2 atoms/cell) versus the grid spacing. For clarity, the total energy obtained with the considered finest grid space (0.10 Å) is selected as the reference.

Note that only the difference between the pseudopotential and the pure Coulomb potential is how to evaluate the local ionic potential $V^k_{\rm loc}$ at $G = 0$. The local ionic potential, $V^k_{\rm loc}$ at $G = 0$, can be estimated by

$$V^k_{\rm loc}(G=0) = 4\pi \int_0^{\infty} \left(V^k_{loc}(r) - (-\frac{Z_k}{r}) \right) r^2 dr, \tag{9}$$

where $V^k_{\rm loc}(r)$ and Z_k are the local pseudopotential and the number of the valence electrons of the kth atomic species, respectively. Because

$$V^k_{\rm loc}(r) = -\frac{Z_k}{r} \qquad (r > r^k_c), \tag{10}$$

the local ionic potential $V^k_{\rm loc}$ at $G = 0$ can be rewritten as

$$V^k_{\rm loc}(G=0) = 4\pi \int_0^{r^k_c} \left(V^k_{loc}(r) + \frac{Z_k}{r} \right) r^2 dr. \tag{11}$$

Therefore, $V_{i-e}(\boldsymbol{G})$ can be determined by Eqs. (6) and (8).

The detailed processes for evaluating $V_{i-e}(\boldsymbol{G})$ are summarized as follows.

(i) Evaluate $\rho_k(r)$ and $V^k_{loc}(G = 0)$ via Eqs. (3) and (11), and store them in pseudopotential files before OF-DFT calculations.
(ii) Estimate the total ionic charge density, $\rho_I(r)$, by Eq. (4) with known $\rho_k(r)$ and structural information.
(iii) Calculate $V_{i-e}(\boldsymbol{G} = 0)$ and $V_{i-e}(\boldsymbol{G} \neq 0)$ by Eq. (8) with $V^k_{\rm loc}(G = 0)$ and Eq. (6) with $\rho_I(\boldsymbol{r})$, respectively.

Once $V_{i-e}(\boldsymbol{G})$ is known, the ion–electron potential in real space, $V_{i-e}(\boldsymbol{r})$, can be obtained by an inverse FFT,

$$V_{i-e}(\boldsymbol{r}) = FFT'(V_{i-e}(\boldsymbol{G})). \tag{12}$$

Note that parallel algorithm of our proposed expression may be not easily achieved for large massively parallel architectures because of the employment of FFTs in our method.

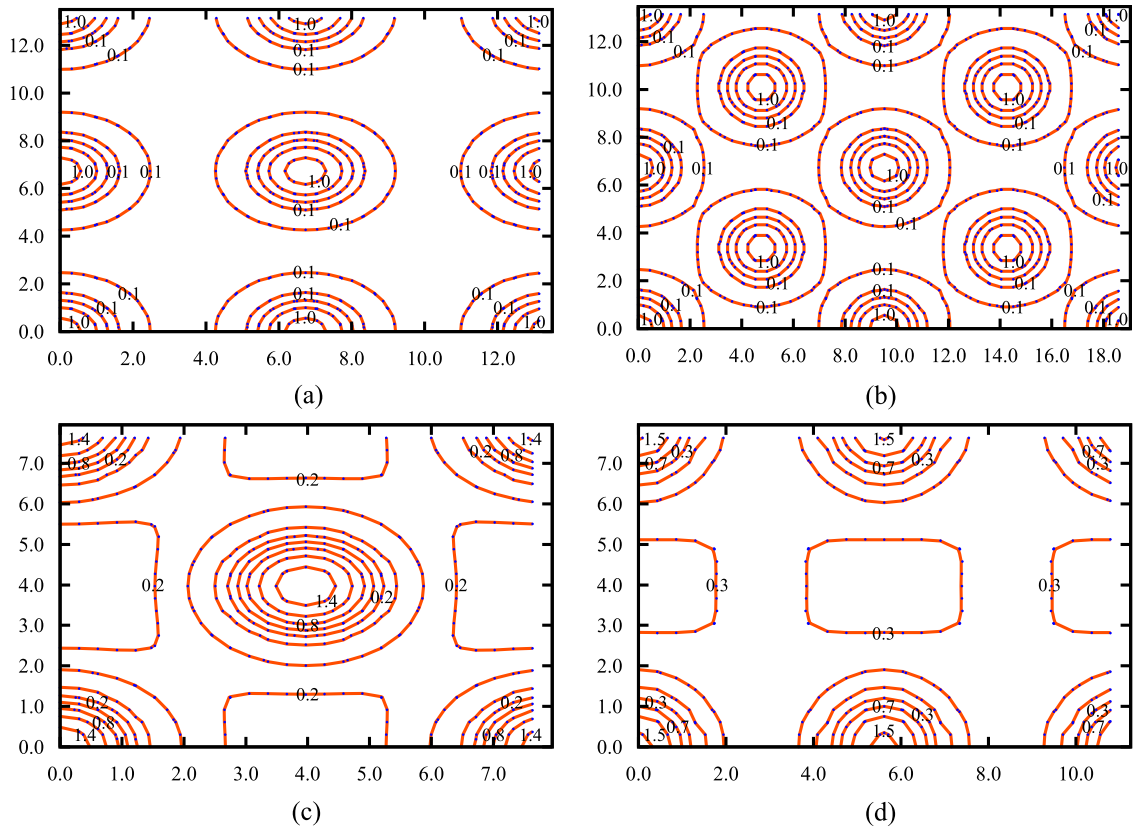

FIG. 4. Contour plots on the uniform grid of ion–electron potential calculated based on the new method (red solid line) and the conventional method (blue dotted line). (a) (001) and (b) (110) planes of Mg with $2 \times 2 \times 2$ bcc unit cells, (c) (001) and (d) (110) planes of Al_3Mg with fcc unit cells. Ion–electron potential and lattice vectors are given in a.u.

22 January 2024 16:56:14

III. NUMERICAL RESULTS

To verify the equivalence of the present scheme to the conventional reciprocal-space method, we coded it into *Ab initio* orbiTaL-free density functionAl theory Software (ATLAS)[7] and benchmarked it with bulk Mg with a body-centered cubic (bcc) lattice. The TF+λvW kinetic energy density functional and the local density approximation exchange–correlation functional parametrized by Perdew and Zunger[19] are used. The local pseudopotential of Mg is constructed by our OEPP scheme,[20] which considers a valence electronic configuration of $3s^1 3p^1$. The core cutoff radius of Mg is set as 2.6 a.u.[20] The ion–ion energy is calculated via Ewald summation.[13]

Fig. 3 shows that the fourth-order finite-difference expansion and a grid spacing of 0.17 Å are sufficient to converge the total energy to well within 1 meV/atom. Therefore, these settings are employed in all the following calculations. Note that a time-saving double-grid technique[21] is adopted to accurately estimate the total ionic charge density for each grid in the unit cell by each pseudo-charge density, which is stored in pseudopotential files. The dense grid-spacing is set as $h_\alpha^{dens} = h_\alpha/2$, and h_α ($\alpha = x, y,$ and z) is the coarse grid-spacing. Ninth-order Lagrangian interpolation is used to obtain the total ionic charge density of the coarse grid.

To validate the new scheme, we compare its calculation of an ion–electron potential with that of a conventional method using structure factor. The resulting contour plots of the ion–electron potential of bcc Mg and face-centered cubic (fcc) Al_3Mg on the (001) and (110) planes are shown in Fig. 4. The negligible difference of ion–electron potential obtained by two methods demonstrates the accuracy of the new scheme. For further benchmarking our proposed method, the bulk properties of hexagonal close-packed Mg, fcc Al and Al_3Mg are calculated and compared with those obtained by the CASTEP code[22] within KS-DFT. Note that the equilibrium volume and bulk modulus B_0 of the studied here were determined by fitting the total energies as a function of volume to the Keane equation of states.[23] The calculated equilibrium volume V_0, total energy E_0, and bulk modulus B_0 are listed in Table I. It is clear that the calculated V_0, E_0, and B_0 are in excellent agreement with the KS-DFT data. This lends a strong support on the validity of our method.

Furthermore, we have calculated the total energies of supercell structures of bcc Mg with different system sizes (up to 8000 atoms) using OF-DFT within the ion-electron potential calculated by the new method and conventional method. The testing results are shown in Table II. The energy difference is constant and negligible with increasing the system sizes. Obviously, the accuracy of our proposed method is independent of the system sizes.

TABLE I. Bulk properties obtained by OF-DFT: equilibrium volume (V_0 per atom in Å^3), total energy (E_0 in eV per atom), and bulk moduli (B_0 in GPa). The data of KS-DFT and kinetic energy density functional parameters of our OF-DFT calculations are adapted from Ref. 7. Note that the new scheme and conventional method are employed to evaluate the ion–electron potential in OF-DFT and KS-DFT, respectively.

Systems	Methods	V_0	E_0	B_0
Mg	KS-DFT	22.023	−24.588	36.5
	Our work	21.902	−24.595	32.6
Al	KS-DFT	18.029	−56.799	69.4
	Our work	18.483	−56.795	66.9
Al_3Mg	KS-DFT	19.031	−48.767	55.2
	Our work	19.008	−48.751	57.0

TABLE II. The total energies (E in eV per atom) of supercell structures of bcc Mg with different system sizes are calculated by OF-DFT, in which the ion-electron potential is obtained by new method and conventional method, and the corresponding energy differences are also included.

System size	100	1000	4000	8000
E obtained by new method	24.4074	24.4074	24.4075	24.4075
E obtained by conventional method	24.4028	24.4028	24.4028	24.4028
Energy difference	0.0046	0.0046	0.0047	0.0047

To demonstrate the performance of new scheme, the ion–electron potential of bulk bcc Mg supercells containing different numbers of atoms (up to 12 000 atoms) was calculated by using the new approach and the conventional method within structure factor. The total calculations times using these two methods are shown in Fig. 5. Compared to conventional method, the new approach shows better computational efficiency and approximately linear scaling with a small prefactor. In particular, the computational time required for an Mg supercell containing 12 000 atoms is decreased substantially from ~18 000 *s* for the conventional method to ~316 *s* for the new scheme.

Within this scheme, the computational efficiency of ATLAS[7] is further tested on Mg supercell with a single processor. The total time and its contributions from the time to calculate the ion–electron term and all other terms throughout the electron density optimizations are presented in Fig. 6 for systems containing 100–12 000 atoms. The computational costs show approximately linear scaling with the number of atoms, because the new scheme is employed to calculate the ion–electron potential term. The proportion of time spent calculating the ion–electron term is trivial, and does not

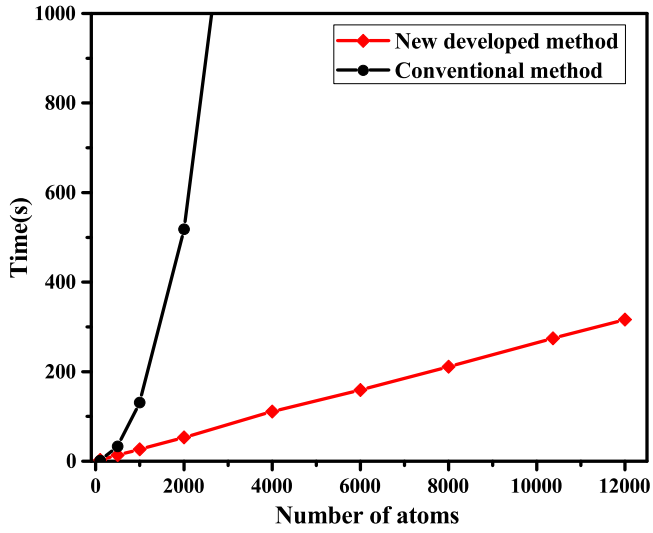

FIG. 5. Total time (wall time) to calculate the ion–electron potential term for different numbers of atoms with the conventional method (black line) and the new method (red line).

22 January 2024 16:56:14

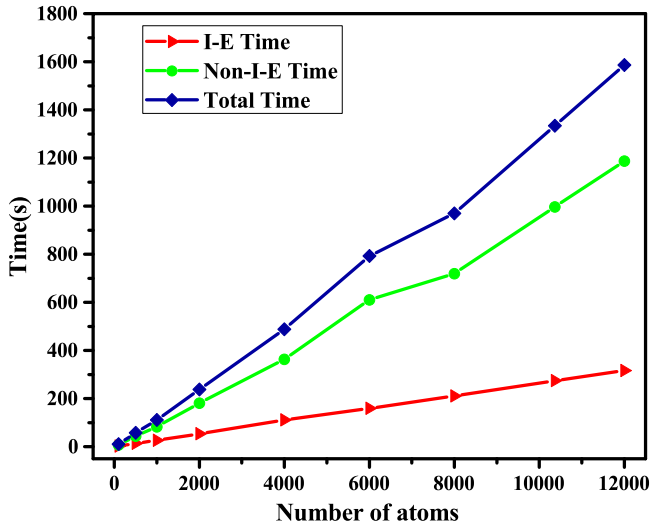

FIG. 6. Total time (wall time) using the new method with ATLAS to calculate the total energy during electron-density optimization for systems of 100–12 000 atoms in a simulated bcc Mg cell. The total time (blue line) is shown as the sum of the times for the ion–electron potential term (red line) and for all other potential and energy terms (green line).

dominate the total computational time within the new scheme. In this regard, our new scheme can greatly improve the computational efficiency of ATLAS the software, and could be applied to large-scale OF-DFT simulations. It is noteworthy that our method can also be used to reduce the computation time for the ion–electron term in KS-DFT simulations, albeit the time spent calculating the ion–electron term of KS-DFT does not dominate the total computational time.

IV. CONCLUSION

In summary, an alternative simple expression for calculating the ion–electron potential of crystalline solids is proposed. Because the expression does not require evaluation of the structure factor for periodic systems, our approach shows $\mathcal{O}(N \log N)$ scaling and can effectively overcome the limitation of high computational cost of conventional approaches. Therefore, it is well suited to simulating large-scale systems within OF-DFT. The method is implemented in ATLAS software and benchmarked using bcc Mg containing large numbers of atoms per unit cell (up to 12 000 atoms). The results show that our method can achieve high computational accuracy and efficiency.

ACKNOWLEDGMENTS

Y.M., Y.W., X.S., and W.M. acknowledge the funding support from the National Natural Science Foundation of China under Grant Nos. 11274136, 11404128, and 11534003, the National Key Research and Development Program of China under Grants No. 2016YFB0201200, the 2012 Changjiang Scholar of the Ministry of Education, the National Key Laboratory of Shock Wave and Detonation Physics, and the China Postdoctoral Science Foundations (Grant Nos. 2015T80294 and 2014M551181). A part of the calculations were performed in the high performance computing center of Jilin University and at Tianhe2-JK in the Beijing Computational Science Research Center.

[1] P. Hohenberg and W. Kohn, Phys. Rev. **136**, B864 (1964).
[2] W. Kohn and L. J. Sham, Phys. Rev. **140**, A1133 (1965).
[3] M. C. Payne, M. P. Teter, D. C. Allan, T. Arias, and J. Joannopoulos, Rev. Mod. Phys. **64**, 1045 (1992).
[4] Y. A. Wang and E. A. Carter, in *Theoretical Methods in Condensed Phase Chemistry* (Springer, 2002), pp. 117–184.
[5] T. A. Wesolowski and Y. A. Wang, *Recent Progress in Orbital-free Density Functional Theory* (World Scientific, 2013).
[6] G. S. Ho, V. L. Lignères, and E. A. Carter, Comput. Phys. Commun. **179**, 839 (2008).
[7] W. Mi, X. Shao, C. Su, Y. Zhou, S. Zhang, Q. Li, H. Wang, L. Zhang, M. Miao, Y. Wang, and Y. Ma, Comput. Phys. Commun. **200**, 87 (2016).
[8] E. Wigner and F. Seitz, Phys. Rev. **46**, 509 (1934).
[9] E. P. Wigner and F. Seitz, *On the Constitution of Metallic Sodium. II* (Springer, Berlin, Heidelberg, 1997), pp. 509–524.
[10] K. Fuchs, Proc. R. Soc. London, Ser. A **151**, 585 (1935).
[11] J. Ihm, A. Zunger, and M. L. Cohen, J. Phys. C: Solid State Phys. **12**, 4409 (1979).
[12] J. Pask and P. Sterne, Phys. Rev. B **71**, 113101 (2005).
[13] P. P. Ewald, Ann. Phys. **369**, 253 (1921).
[14] T. Darden, D. York, and L. Pedersen, J. Chem. Phys. **98**, 10089 (1993).
[15] U. Essmann, L. Perera, M. L. Berkowitz, T. Darden, H. Lee, and L. G. Pedersen, J. Chem. Phys. **103**, 8577 (1995).
[16] L. Hung and E. A. Carter, Chem. Phys. Lett. **475**, 163 (2009).
[17] M. Frigo and S. G. Johnson, in *Proceedings of the 1998 IEEE International Conference on Acoustics, Speech and Signal Processing* (IEEE, 1998), Vol. 3, pp. 1381–1384.
[18] R. M. Martin, *Electronic Structure: Basic Theory and Practical Methods* (Cambridge University Press, 2004).
[19] J. P. Perdew and A. Zunger, Phys. Rev. B **23**, 5048 (1981).
[20] W. Mi, S. Zhang, Y. Wang, Y. Ma, and M. Miao, J. Chem. Phys. **144**, 134108 (2016).
[21] T. Ono and K. Hirose, Phys. Rev. Lett. **82**, 5016 (1999).
[22] S. J. Clark, M. D. Segall, C. J. Pickard, P. J. Hasnip, M. I. Probert, K. Refson, and M. C. Payne, Z. Kristallogr. - Cryst. Mater. **220**, 567 (2005).
[23] A. Keane, Aust. J. Phys. **7**, 322 (1954).

22 January 2024 16:56:14